arXiv:2605.07186v1 [cs.CL] 8 May 2026

The Text Uncanny Valley: Non-Monotonic Performance Degradation in LLM Information Retrieval

Zekai Tong[1,*] **Ruiyao Xu**[2] **Aryan Shrivastava**[1]
Chenhao Tan[1] **Ari Holtzman**[1]
[1]University of Chicago [2]Northwestern University

Abstract

Existing Large Language Model (LLM) benchmarks primarily focus on syntactically correct inputs, leaving a significant gap in evaluation on imperfect text. In this work, we study how word-boundary corruption affects how LLMs detect targeted information. By inserting whitespace characters within words to break them into fragments, LLMs' detection accuracy follows a **U-shaped curve** with the increase in insertion rate. We refer to this curve as the **Text Uncanny Valley**. To explain such observation, we propose a *mode transition* hypothesis: LLMs operate in a word-level mode for near-normal text and a character-level mode for heavily fragmented text, with the valley marking the disordered transition where neither mode is effective. Four experiments and one analysis are consistent with this account: in-context learning fails to rescue valley-bottom performance; regularizing the perturbation substantially reduces the U-shape; a math reasoning task replicates the U-shape for Gemini 3.0 Flash but not for stronger models, suggesting the effect is attenuated when tasks rely less on exact lexical alignment; and tokenization entropy peaks before the F1 minimum, consistent with a regime-conflict interpretation. These findings reveal a failure mode invisible to clean-text benchmarks yet directly relevant to any deployment scenario involving noisy or uncurated text inputs.

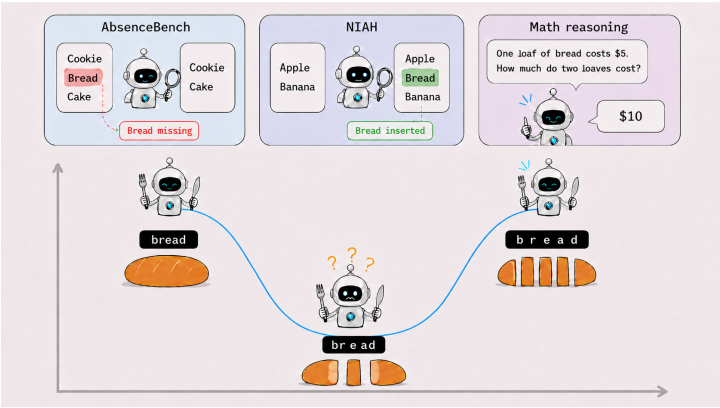

Figure 1: Bread slicing as an analogy for our text fragmentation method and the resulting Text Uncanny Valley phenomenon. We evaluate three tasks: AbsenceBench, NIAH-style task, and math reasoning. Image generated by ChatGPT.

[1]*Corresponding author: zekaitong@uchicago.edu

Preprint.

1 Introduction

Large language models (LLMs) are increasingly deployed in settings where input text is far from clean. Documents extracted from PDFs via optical character recognition (OCR), content copy-pasted from web pages, and outputs from automated pipelines routinely contain formatting artifacts, including spurious spaces inserted within words (e.g. *international* $\rightarrow$ *int er nation al*). Such corruption occurs routinely in any system that processes uncurated text, but no existing benchmark measures its effect on LLM performance. Although recent work has begun to evaluate LLM robustness under noisy text [Singh et al., 2024, Agrawal et al., 2025, Piryani et al., 2025], none examine how word-boundary corruption on tasks that demand *exact* span-level matching between two document versions, where tokenization disruption has the most room to cause damage.

To address this gap, we study two complementary evaluation tasks: **absence detection** [Fu et al., 2025], where models identify deliberately omitted lines, and a **NIAH-style** task [Kamradt, 2023], where models identify inserted lines. Both tasks require a model to align two document versions at the line level, making them sensitive to any corruption that disrupts word boundaries. To study this sensitivity in a controlled way, we insert spaces inside words at a tunable rate $\texttt{word_fragmentation_rate} \in [0, 1]$, sweeping from clean text ($\texttt{word_fragmentation_rate} = 0$) to fully character-separated text ($\texttt{word_fragmentation_rate} = 1$) across eleven levels and three domains, including legal contracts, GitHub PRs, and mathematical reasoning.

The most intuitive expectation is monotonic degradation: more corruption, worse performance. What we observe instead is a **non-monotonic U-shaped** performance curve across the strongest model families: Micro-F1 degrades as fragmentation increases, reaches a minimum at moderate rates, and then partially *recovers* at extreme fragmentation. We call this the **Text Uncanny Valley** [Mori, 1970, Seyama and Nagayama, 2007]: text that is neither fully natural nor uniformly fragmented leaves the model in a disordered in-between state where performance is worst.

We evaluate eight model variants across three domains. Three families, Gemini 3.0 Flash [Google, 2025], GPT-5.2 [OpenAI, 2025], and Claude 4.5 Haiku [Anthropic, 2025], consistently exhibit the U-shape on both tasks and are the focus of subsequent analysis. That performance *recovers* at high fragmentation, rather than continuing to degrade, rules out a simple "more noise, worse performance" account and points to a shift in how the model processes text. We then formalize this as a *two-regime hypothesis*: LLMs rely on word-level processing for near-normal text and fall back to character-level processing for heavily fragmented text, with the valley marking the unstable transition between the two. Four experiments and a tokenization entropy analysis test this account.

Our contributions can be summarized into four folds:

- **Benchmark.** A controlled `word_fragmentation_rate` perturbation framework that sweeps word-boundary corruption from clean text to fully character-separated text across eleven levels, evaluated on two span-matching tasks and three domains.
- **Phenomenon.** Three of eight model families, Gemini 3.0 Flash, GPT-5.2, and Claude 4.5 Haiku, exhibit a consistent U-shaped performance curve on both tasks, which we name the Text Uncanny Valley.
- **Explanation.** We propose a two-regime hypothesis and provide converging evidence: ① ICL cannot rescue valley-bottom performance; ② regularizing fragmentation reduces the U-shape while inter-word whitespace manipulation does not induce it; ③ tokenization entropy peaks before the F1 minimum; ④ a math reasoning control shows the effect is attenuated without cross-document alignment.
- **Implication.** Moderate word-boundary corruption, the level typical of OCR artifacts, is more damaging than extreme corruption, a failure mode invisible to clean-text benchmarks.

2 Related Work

Absence detection and NIAH. Fu et al. [2025] establish that LLMs fail at absence detection on clean text, achieving only around 70% Micro-F1 despite near-perfect scores on NIAH retrieval [Kamradt, 2023, Hsieh et al., 2024]. We replicate and extend their evaluation to fragmented text. Jain and Garimella [2026] and Ming et al. [2025] study related but distinct problems where missing information is semantically defined; neither examines text-level corruption.

LLM robustness to text perturbation. Singh et al. [2024] and Zhuo et al. [2025] benchmark LLMs under OCR errors, typos, and character-level perturbations; both find that models tolerate mild noise but degrade under heavier corruption. Sclar et al. [2024] show spacing variations can shift accuracy by up to 76 points. Pawar et al. [2025] study tokenizer-induced word splitting. Our key distinction: prior work reports monotonic degradation; we reveal a *non-monotonic* pattern where moderate fragmentation is worse than extreme, via continuous rate sweeps that expose a recovery regime discrete evaluations miss.

Other U-shaped curves in LLMs. Liu et al. [2024] document a U-shape as a function of information *position*; ours arises from intra-word fragmentation, a different axis and mechanism.

Tokenization and word boundaries. Alqahtani et al. [2026] argue tokenization is a core modeling decision; Chai et al. [2024] show LLMs remain brittle to typographical variations under BPE [Sennrich et al., 2016]—a pattern we extend to continuous intra-word space insertion with non-monotonic effects.

In-context learning under noise. Gao et al. [2024] and Jiao et al. [2026] show corrupted demonstrations can hurt or mislead ICL, grounding our observation that ICL fails to rescue valley-bottom performance.

3 Method: Controlled Word-Boundary Fragmentation

3.1 Perturbation Design

We perturb documents by inserting spaces within words. For each *contiguous non-space character sequence*, we iterate over its *intra-word slots* (positions between adjacent characters). A sequence of k characters has $k-1$ slots; `cat` has 2 slots, so inserting at the first yields `c at` with `word_fragmentation_rate` $= \frac{1}{2}$. At each slot, we insert a space with probability $p \in [0, 1]$. The degree of perturbation is measured by the **word fragmentation rate** (`word_fragmentation_rate`), defined as:

$$\texttt{word_fragmentation_rate} = \frac{\text{number of spaces actually inserted}}{\text{total number of intra-word slots}} \tag{1}$$

Because insertion is stochastic, the measured `word_fragmentation_rate` may differ slightly from p, though in practice the difference is negligible.[1] We sweep `word_fragmentation_rate` across eleven levels: $\{0.0, 0.1, 0.2, \ldots, 1.0\}$. Appendix E.3 illustrates the effect on a legal document excerpt at representative `word_fragmentation_rate` levels.

Two design properties make this perturbation suitable for controlled experimentation:

- **Continuous.** `word_fragmentation_rate` sweeps from 0.0 (clean input) to 1.0 (every character pair separated by a space), providing a fine-grained view of how word-boundary integrity interacts with model capability.
- **Separable.** The target seed (which lines are omitted or inserted) and the fragmentation seed (where spaces are inserted) are independently controlled. Target masks are fixed across all fragmentation rates, ensuring that task difficulty does not covary with the perturbation level.

3.2 Datasets

We evaluate on three domains, each with distinct textual characteristics.

Legal documents. We use CUAD-QA [Hendrycks et al., 2021], expert-annotated commercial contracts from the EDGAR filing system. Dense natural-language prose makes these documents highly sensitive to word-boundary disruption.

GitHub pull requests. We use the same corpus as Fu et al. [2025]: code diffs containing long non-spaced identifier runs (e.g., `getUserByEmailAndPassword`), making the text structurally dense before any perturbation.

[1] Since the measured `word_fragmentation_rate` is nearly identical to p across all experiments, we use p to denote the fragmentation level but retain `word_fragmentation_rate` as the x-axis label for notational convenience.

Mathematical reasoning (GSM8K). We draw problems from GSM8K [Cobbe et al., 2021], a dataset of 8,500 grade-school math word problems with step-by-step solutions, created by OpenAI.[2] To create documents of sufficient length to challenge modern LLMs, we concatenate 80 problems per document, a volume approximating two weeks of student homework. Each question and its solution are treated as a sequence of lines split by periods and newlines. The resulting document structure is illustrated in Appendix E.1.

Due to the substantial computational cost of our evaluation protocol (see Appendix A for details), we sample 100 documents per domain.

3.3 Evaluation Tasks

We evaluate word-boundary fragmentation on two tasks, both requiring exact span-level matching between document versions.

Absence detection. Following Fu et al. [2025], each instance provides both the original document and a version from which lines have been deleted; the model must identify exactly which lines are missing. This task requires exact lexical alignment and is highly sensitive to intra-word disruption. The prompt template is in Appendix E.2.

NIAH-style insertion detection. Each instance provides both the original document and a version into which extra lines have been inserted; the model must identify exactly which lines were added. This adapts the classic NIAH setup [Kamradt, 2023] to require span matching rather than simple retrieval, and uses the same Micro-F1 metric. The prompt template and full experimental details are in Appendix C.

Following Fu et al. [2025], both tasks are evaluated using Micro-F1 based on case-insensitive exact matching per line. This metric effectively penalizes false positives, providing a more rigorous assessment than recall alone.

Since we find that varying the omission/insertion rate does not substantially alter the U-shaped curve, we fix the omission/insertion rate at $p = 0.1$ for both tasks. All models are queried via their respective APIs. Model responses are parsed to extract the list of predicted target lines, which are then compared against the ground-truth to compute Micro-F1.[3]

4 The Text Uncanny Valley

4.1 Main Finding: The U-shaped Curve and the Text Uncanny Valley

We evaluate eight model variants: DeepSeek-V3 [DeepSeek-AI, 2024], Grok-4.1-Fast [xAI, 2025], Qwen3-Plus [Yang et al., 2025], Gemini 3.0 Flash (standard and thinking) [Google, 2025], GPT-5.2 (standard and thinking) [OpenAI, 2025], and Claude 4.5 Haiku [Anthropic, 2025]. Among these, only Gemini 3.0 Flash, GPT-5.2, and Claude 4.5 Haiku exhibit a clear and consistent non-monotonic U-shaped curve across both tasks. Grok-4.1-Fast shows largely monotonic decline without a discernible rebound. Qwen3-Plus exhibits irregular curve shapes, generally poor performance, and slow API responses with high cost, making it unsuitable for further analysis. DeepSeek-V3 performs poorly throughout and frequently produces invalid outputs at high fragmentation rates. Full results for all eight variants are provided in Appendix D. The remainder of this paper focuses on the three model families that consistently exhibit the Text Uncanny Valley.[4]

The Text Uncanny Valley. We name this non-monotonic curve the **Text Uncanny Valley** [Mori, 1970, Seyama and Nagayama, 2007]: just as human affinity drops for robots that are nearly but not perfectly realistic, LLMs enter a disordered transitional state when processing text that is neither fully natural nor uniformly fragmented. The Micro-F1 drop predominantly reflects genuine detection failures rather than a formatting artifact.

[2] `https://huggingface.co/datasets/openai/gsm8k`

[3] Full implementation and parsing details are provided in Appendix E.

[4] GPT-5.2 returned API errors on a small number of documents in some conditions due to context length limits; affected documents were excluded from the corresponding averages.

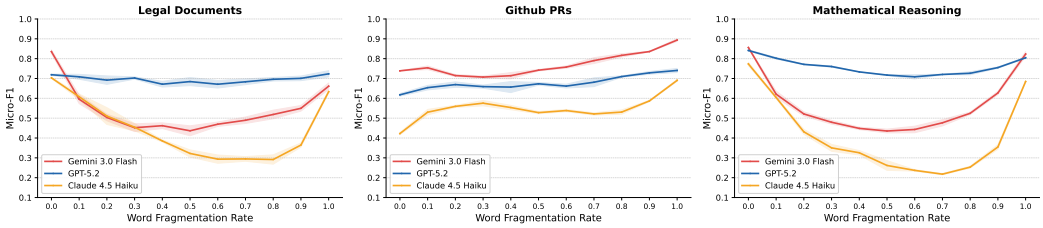

Figure 2: **The Text Uncanny Valley**: Micro-F1 vs. `word_fragmentation_rate` for absence detection on Legal Documents (left), GitHub PRs (centre), and Mathematical Reasoning (right). Shaded bands: ± 1 std over three fragmentation seeds.

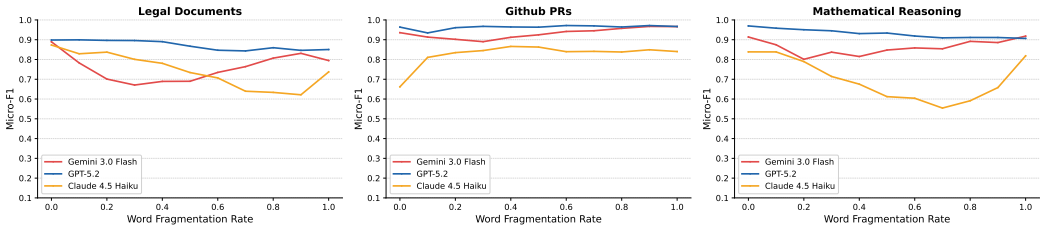

Figure 3: NIAH-style insertion detection under fragmentation. Results for the same domains and models as Figure 2. While the U-shaped **Text Uncanny Valley** remains present, the effect is less pronounced than in the absence detection task.

The U-shaped curve appears in both tasks, but is more pronounced in absence detection than in NIAH-style insertion detection. Since the effect is clearest in absence detection, the follow-up experiments in Section 5 use absence detection as the primary testbed.

4.2 Variation Across Domains and Models

Although all three models exhibit a U shape across all domains in absence detection, and in most cases for NIAH, the curve varies substantially with both the domain and the model family.

GitHub PRs vs. natural-language domains. On Legal Documents and Mathematical Reasoning, all three models follow the expected U-shape from the clean baseline in absence detection. On GitHub PRs, however, all three models show an initial *rise* in Micro-F1 at low `word_fragmentation_rate` before turning downward. GitHub PR diffs are already dense with long non-spaced identifier runs, and a small number of inserted spaces may help by breaking these into shorter, more parseable units before heavier fragmentation overwhelms this benefit. This initial rise pattern appears in absence detection and for Claude 4.5 Haiku in NIAH, suggesting it reflects domain structure.

Legal Documents vs. Mathematical Reasoning. In most cases, the valley is noticeably deeper on Mathematical Reasoning than on Legal Documents, suggesting the effect is amplified when lines share strict logical dependencies.[5]

Model comparison. Across both tasks, GPT-5.2 consistently produces the flattest curve and achieves the highest absolute Micro-F1 in most settings, suggesting greater robustness to word-boundary fragmentation. Claude 4.5 Haiku shows the deepest valley in absence detection, with its valley bottom noticeably right-shifted relative to the other two models; this pattern is less prominent in NIAH, possibly because the insertion detection task is overall less sensitive to the transition zone. Gemini 3.0 Flash falls between the two in most cases.

[5]Establishing a causal link would require controlled experiments varying dependency structure, which we leave to future work.

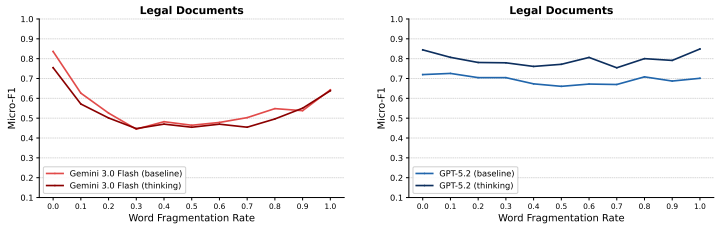

Figure 4: Comparison of standard and thinking mode on legal documents for Gemini 3.0 Flash (left) and GPT-5.2 (right).

4.3 Thinking Mode Does not Consistently Help

Fu et al. [2025] report a 7.9% thinking-mode boost on clean text. We test whether this extends to fragmented text, evaluating Gemini 3.0 Flash and GPT-5.2 on Legal Documents under absence detection (which shows the stronger U-shape; NIAH evaluation is left to future work).

Figure 4 shows the results. The U-shaped curve persists in both thinking-mode variants, but the effect differs markedly between models. Gemini 3.0 Flash thinking mode fails to improve performance in most conditions and sometimes performs worse than the baseline. GPT-5.2 thinking mode consistently improves Micro-F1 across fragmentation rates, though it does not eliminate the valley. Given the substantial increase in latency and cost, the cost-benefit tradeoff of thinking mode is unfavorable in this setting, at least for Gemini.[6]

5 Hypothesis: Two Processing Modes

The recovery at high fragmentation rules out a simple "more noise, worse output" account: if fragmentation only destroyed information, performance would decline monotonically. That performance *rebounds* means the model at `word_fragmentation_rate` $= 1.0$ operates in a qualitatively different state than at `word_fragmentation_rate` $= 0.5$. What changes between these two points is the tokenizer's output. At low `word_fragmentation_rate`, subword tokenizers produce familiar multi-character tokens and the model reasons over words as coherent units. At `word_fragmentation_rate` $= 1.0$, every character is space-separated, collapsing the vocabulary to near-uniform single-character tokens; the model falls back to character-level pattern matching, a regime where "word recovery" has been independently documented [Yang et al., 2026]. Both extremes are internally consistent. The problem arises at intermediate `word_fragmentation_rate`, where words are inconsistently affected: while some remain intact, others are partially or fully shattered into irregular fragments; the model cannot commit to either processing strategy.

Two-Regime Hypothesis

LLMs process text in two regimes:

1. **Word-level regime** (`word_fragmentation_rate` ≈ 0): subword tokenization is stable; the model aligns and compares documents through lexical units.
2. **Character-level regime** (`word_fragmentation_rate` ≈ 1): tokenization collapses to single characters; the model effectively operates on character patterns to recover semantics.

The *Text Uncanny Valley* is the transition zone where tokenization is neither coherently subword nor uniformly character-level, and neither strategy is effective.

This hypothesis yields testable predictions: if the bottleneck is tokenization level, prompt level interventions such as in-context learning should not resolve it; if it is the *irregularity* of fragmentation that triggers the valley, then more regular fragmentation patterns should substantially reduce or eliminate it; and if the valley marks a transition between two tokenization regimes, then tokenization heterogeneity should peak near the same region as the F1 minimum.

[6]We do not extend thinking-mode evaluation beyond Gemini 3.0 Flash and GPT-5.2 on Legal Documents; broader evaluation is a direction for future work.

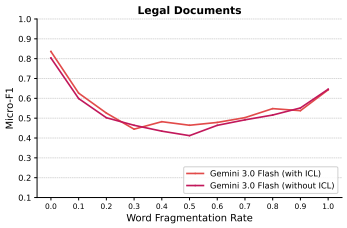

Figure 5: Effect of ICL on Micro-F1 across fragmentation rates for Gemini 3.0 Flash on legal documents. The U-shaped curve persists with and without ICL.

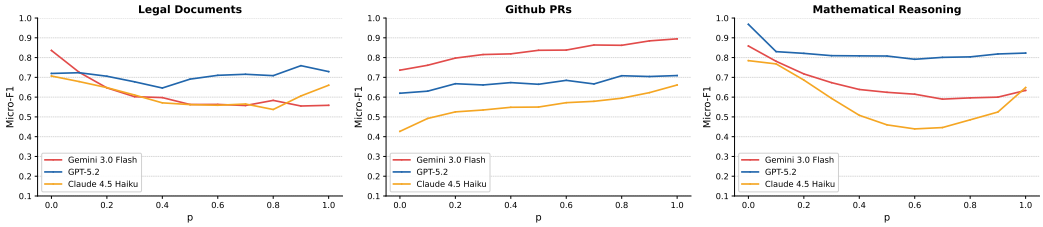

Figure 6: Fixed-slot fragmentation results across three domains. In the fixed-slot condition, a space is inserted at the first slot of each contiguous non-space character sequence with probability p. Each panel shows Micro-F1 as a function of p for Gemini 3.0 Flash, GPT-5.2, and Claude 4.5 Haiku.

5.1 ICL Cannot Rescue the Valley

Setup. If the valley arises from a lack of task strategy, providing few-shot examples of correctly handled fragmented text should help. We prepend 3 such examples to the prompt (see Appendix E.4 for the full template) and rerun evaluation on **absence detection** across all fragmentation rates.[7]

Results. As shown in Figure 5, the U-shaped curve persists after ICL with shape and valley position largely unchanged. ICL yields no significant performance improvement in most conditions and in several conditions leads to a measurable performance decrease, consistent with findings that corrupted demonstrations can mislead rather than guide models [Gao et al., 2024, Jiao et al., 2026]. The bottleneck is therefore not accessible to prompt level intervention, suggesting that the valley arises from tokenization level processing rather than from a lack of appropriate task strategy.

> **Finding 1: the bottleneck is below the prompting level**
>
> ICL does not rescue valley-bottom performance. The valley's position and shape are unchanged, ruling out task comprehension as the limiting factor.

5.2 Fixed-slot Fragmentation Substantially Reduces the U-shape

Setup. We compare random-slot fragmentation against a **fixed-slot** variant that inserts a space at the *first slot only* of each contiguous non-space character sequence with probability p; no spaces are inserted at any other slot within the same sequence.[8] This imposes a more regular, predictable insertion pattern.[9]

Results on Legal Documents and Mathematical Reasoning. Fixed-slot fragmentation substantially reduces the U-shape on both natural-language domains (Figure 6). Gemini 3.0 Flash plateaus without

[7] Due to computational constraints, ICL evaluation is conducted on Gemini 3.0 Flash on Legal Documents. Broader evaluation is left to future work.

[8] p and `word_fragmentation_rate` are distinct: p is the probability of inserting a space after the first intra-word slot of each contiguous non-space character sequence, while `word_fragmentation_rate` measures the fraction of *all* intra-word slots that received a space across the entire document; the same p yields different `word_fragmentation_rate` values depending on token-length distribution.

[9] Our codebase also supports inserting at the n-th slot or m-th percentile slot of each sequence; we leave systematic evaluation of these variants to future work.

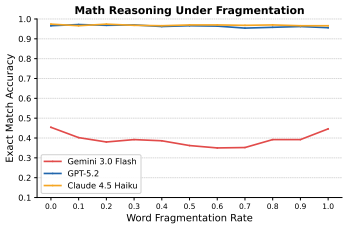

Figure 7: Math reasoning accuracy on individual GSM8K problems vs. `word_fragmentation_rate`. Thinking mode is disabled. Gemini 3.0 Flash shows a clear U-shape; GPT-5.2 and Claude 4.5 Haiku remain near ceiling.

a rebound; GPT-5.2 shows a similar pattern on Mathematical Reasoning but no clear trend on Legal Documents. Claude 4.5 Haiku still shows a partial uptick at high p, though less pronounced than under random-slot.

Results on GitHub PRs. Surprisingly, all three models show monotonically *increasing* Micro-F1: regular space insertion breaks dense identifier runs into shorter units, consistently helping the model.

Interpretation. These results support the two-modes hypothesis via two mechanisms. First, regular fragmentation cannot fully activate the character-level regime at $p = 1.0$, so no rebound occurs. Second, it avoids the chaotic mixed tokenization state: the model adapts to a predictable structure rather than oscillating between regimes. The GitHub PRs inversion confirms that the valley is driven not by the amount of fragmentation, but by the disorder it introduces; regularizing this density eliminates the valley in natural language and actively assists the model on dense code diffs.

Finding 2: irregularity, not magnitude, drives the valley

Regular fragmentation eliminates the rebound on natural-language domains and *monotonically improves* performance on code diffs. The valley arises from *how* text is fragmented, rather than *how much*.

5.3 Inter-word Whitespace Manipulation Does Not Induce the Valley

We conduct a control experiment where inter word spaces are randomly replaced with either two spaces or a space and a tab character. Under this setup, performance remains largely unchanged and no U shaped curve emerges; this confirms that the valley arises from disrupting contiguous non space sequences, rather than from the mere act of inserting whitespace.

Finding 3: intra-word disruption is the cause

Extra whitespace *between* words does not produce the valley. Only breaking apart intra-word character sequences, which disrupts subword tokenization, triggers the effect.

5.4 Math Reasoning under Fragmentation

To test whether the Text Uncanny Valley generalizes beyond absence detection and insert detection, we apply the same fragmentation protocol to a direct math reasoning task [Cobbe et al., 2021], giving each model individual problems at eleven `word_fragmentation_rate` levels and evaluating accuracy (see Appendix B for full details). Gemini 3.0 Flash retains a pronounced U-shaped curve, while GPT-5.2 and Claude 4.5 Haiku remain near ceiling throughout.

Two factors likely explain the contrast: math reasoning does not require exact cross-document lexical alignment, and both inputs and outputs are substantially shorter than in the experiments in Section 4, reducing the surface area for tokenization disruption to accumulate. Both are consistent with the two-modes hypothesis: the U-shape is more pronounced when a task requires the model to operate precisely in the transition zone between word-level and character-level processing.

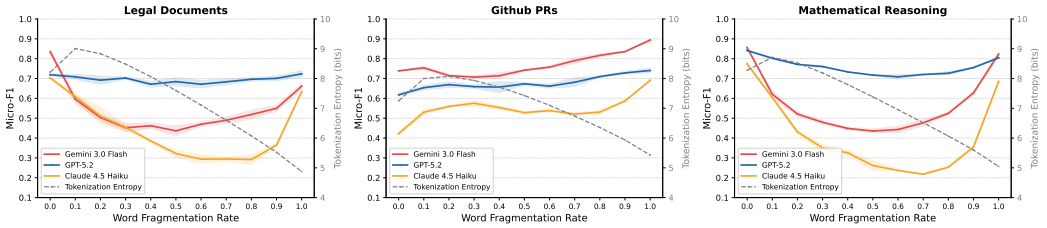

Figure 8: Tokenization entropy (dashed) overlaid on Micro-F1 (solid) from the absence detection experiment, as a function of `word_fragmentation_rate` across three domains. Entropy first rises then falls as `word_fragmentation_rate` increases; the F1 curve follows the inverse shape.

Finding 4: the U-shape is task and model dependent

The valley persists for Gemini 3.0 Flash but disappears for GPT-5.2 and Claude 4.5 Haiku on math reasoning. The effect is strongest when exact cross-document alignment is required over long inputs.

5.5 Analysis: Tokenization Entropy

Setup. We compute the Shannon entropy of the token-ID distribution for each document at each `word_fragmentation_rate` level, using the `cl100k_base` encoding accessed via `tiktoken`.[10]

$$H = -\sum_{t} p(t) \log_2 p(t) \tag{2}$$

where $p(t)$ is the empirical frequency of token t in the document. High entropy indicates a diverse, heterogeneous token distribution; low entropy indicates dominance by a small vocabulary (e.g., individual letters at high fragmentation). Shannon entropy is a standard measure of distributional diversity [Shannon, 1948].

Results. As shown in Figure 8, tokenization entropy rises then falls as `word_fragmentation_rate` increases across all three domains, forming an inverted U-shape that mirrors the U-shaped F1 curve. Notably, the entropy peak occurs at a lower `word_fragmentation_rate` than the F1 valley, i.e., entropy is already declining by the time performance reaches its minimum.

Interpretation. The entropy peak occurs before the F1 minimum, indicating that maximum tokenization heterogeneity alone does not account for the valley. This offset is consistent with the two-modes hypothesis: the F1 minimum may correspond to a transition region where word-level processing has degraded while character-level processing has not yet stabilized, rather than to the point of maximum tokenization heterogeneity itself. The entropy trajectory thus provides indirect support by showing that the tokenization regime shifts non-monotonically across the fragmentation range.

Finding 5: the valley marks a regime transition

Tokenization entropy peaks *before* the F1 minimum across all three domains. The valley is not the point of maximum token confusion but the no-man's-land between two processing regimes.

6 Conclusion

We document the **Text Uncanny Valley**: under word-boundary fragmentation, LLM performance follows a U-shaped curve on absence detection and NIAH-style insertion detection, reaching its minimum at moderate fragmentation before partially recovering at extremes. This reveals a clean-text-invisible failure mode, especially for tasks requiring exact lexical alignment.

Our analyses support a two-regime account: ICL does not rescue the valley; regularized fragmentation weakens it; inter-word whitespace does not induce it; math reasoning shows the effect is model and

[10] We verified that results are nearly identical whether accessed as `encoding_for_model("gpt-4")` or `get_encoding("cl100k_base")`.

task dependent; and tokenization entropy peaks before the F_1 minimum. Together, these results suggest that the valley marks an unstable transition between word-level and character-level processing.

Moderate word-boundary corruption may therefore be more dangerous than extreme fragmentation for OCR pipelines, document processing systems, and LLM-as-judge evaluators. Future work should study how to mitigate this transition-zone failure mode, and ensure robustness benchmarks cover the ambiguous middle regime between clean and uniformly corrupted text.

Acknowledgements

This work was supported by New Forms of Socio-Cognitive AI Initiative at the University of Chicago.

References

A. Agrawal, L. Alazraki, S. Honarvar, and M. Rei. Enhancing LLM robustness to perturbed instructions: An empirical study. *arXiv preprint arXiv:2504.02733*, 2025. URL https://arxiv.org/abs/2504.02733.

S. Alqahtani, M. T. Nayeem, M. T. R. Laskar, T. Mohiuddin, and M. S. Bari. Stop taking tokenizers for granted: They are core design decisions in large language models. In *Proceedings of the 19th Conference of the European Chapter of the Association for Computational Linguistics (Volume 1: Long Papers)*, pages 8410–8432, 2026. URL https://aclanthology.org/2026.eacl-long.394/.

Anthropic. System card: Claude Haiku 4.5. https://anthropic.com/claude-haiku-4-5-system-card, 2025.

Y. Chai, Y. Fang, Q. Peng, and X. Li. Tokenization falling short: On subword robustness in large language models. In *Findings of the Association for Computational Linguistics: EMNLP 2024*, pages 1582–1599, 2024. URL https://aclanthology.org/2024.findings-emnlp.86/.

K. Cobbe, V. Kosaraju, M. Bavarian, M. Chen, H. Jun, L. Kaiser, M. Plappert, J. Tworek, J. Hilton, R. Nakano, C. Hesse, and J. Schulman. Training verifiers to solve math word problems. *arXiv preprint arXiv:2110.14168*, 2021. URL https://arxiv.org/abs/2110.14168.

DeepSeek-AI. DeepSeek-V3 technical report. *arXiv preprint arXiv:2412.19437*, 2024. URL https://arxiv.org/abs/2412.19437.

H. Y. Fu, A. Shrivastava, J. Moore, P. West, C. Tan, and A. Holtzman. Absence Bench: Language models can't see what's missing. In *The Thirty-ninth Annual Conference on Neural Information Processing Systems Datasets and Benchmarks Track*, 2025. URL https://openreview.net/forum?id=pmLMrqhIpb.

H. Gao, F. Zhang, W. Jiang, J. Shu, F. Zheng, and H. Wei. On the noise robustness of in-context learning for text generation. In *Advances in Neural Information Processing Systems (NeurIPS)*, volume 37, 2024. URL https://arxiv.org/abs/2405.17264.

Google. Gemini 3 flash. https://cloud.google.com/blog/products/ai-machine-learning/gemini-3-flash-for-enterprises, 2025.

D. Hendrycks, C. Burns, A. Chen, and S. Ball. CUAD: An expert-annotated NLP dataset for legal contract review. In *Proceedings of the Neural Information Processing Systems Track on Datasets and Benchmarks*, 2021. URL https://openreview.net/forum?id=7l1Ygs3Bamw.

C.-P. Hsieh, S. Sun, S. Kriman, S. Acharya, D. Rekesh, F. Jia, Y. Zhang, and B. Ginsburg. RULER: What's the real context size of your long-context language models? *arXiv preprint arXiv:2404.06654*, 2024. URL https://arxiv.org/abs/2404.06654.

A. Jain and A. Garimella. Knowing what's missing: Assessing information sufficiency in question answering. In *Findings of the Association for Computational Linguistics: EACL 2026*, pages 4163–4174, 2026.

D. Jiao, D. Wang, and L. Hu. Understanding the dynamics of demonstration conflict in in-context learning. *arXiv preprint arXiv:2603.04464*, 2026.

G. Kamradt. LLMTest_NeedleInAHaystack: Pressure testing LLMs. https://github.com/gkamradt/LLMTest_NeedleInAHaystack, 2023.

N. F. Liu, K. Lin, J. Hewitt, A. Paranjape, M. Bevilacqua, F. Petroni, and P. Liang. Lost in the middle: How language models use long contexts. *Transactions of the Association for Computational Linguistics*, 12:157–173, 2024.

Y. Ming, S. Purushwalkam, S. Pandit, Z. Ke, X.-P. Nguyen, C. Xiong, and S. Joty. FaithEval: Can your language model stay faithful to context, even if "The Moon is Made of Marshmallows"? In *International Conference on Learning Representations*, 2025. URL https://openreview.net/forum?id=UeVx6L59fg.

M. Mori. Bukimi no tani [The Uncanny Valley]. *Energy*, 7(4):33–35, 1970. In Japanese. English translation by Karl F. MacDorman and Norri Kageki, IEEE Robotics & Automation Magazine, 19(2):98–100, 2012.

OpenAI. Update to GPT-5 system card: GPT-5.2. https://openai.com/index/gpt-5-system-card-update-gpt-5-2/, 2025.

S. Pawar, M. Apte, K. Jadhav, G. K. Palshikar, and N. Ramrakhiyani. Broken words, broken performance: Effect of tokenization on performance of LLMs. In *Proceedings of the 14th International Joint Conference on Natural Language Processing and the 4th Conference of the Asia-Pacific Chapter of the Association for Computational Linguistics*, pages 372–385, 2025. URL https://aclanthology.org/2025.ijcnlp-short.31/.

B. Piryani, J. Mozafari, A. Abdallah, A. Doucet, and A. Jatowt. MultiOCR-QA: Dataset for evaluating robustness of LLMs in question answering on multilingual OCR texts. *arXiv preprint arXiv:2502.16781*, 2025. URL https://arxiv.org/abs/2502.16781.

M. Sclar, Y. Choi, Y. Tsvetkov, and A. Suhr. Quantifying language models' sensitivity to spurious features in prompt design or: How I learned to start worrying about prompt formatting. In *Proceedings of the International Conference on Learning Representations (ICLR)*, 2024. URL https://arxiv.org/abs/2310.11324.

R. Sennrich, B. Haddow, and A. Birch. Neural machine translation of rare words with subword units. In *Proceedings of the 54th Annual Meeting of the Association for Computational Linguistics (Volume 1: Long Papers)*, pages 1715–1725, 2016. URL https://aclanthology.org/P16-1162/.

J. Seyama and R. S. Nagayama. The uncanny valley: Effect of realism on the impression of artificial human faces. *Presence: Teleoperators and Virtual Environments*, 16(4):337–351, 2007.

C. E. Shannon. A mathematical theory of communication. *The Bell System Technical Journal*, 27(3): 379–423, 1948.

A. Singh, N. Singh, and S. Vatsal. Robustness of large language models to perturbations in text. *arXiv preprint arXiv:2407.08989*, 2024. URL https://arxiv.org/abs/2407.08989.

xAI. Grok 4.1 Fast and Agent Tools API. https://x.ai/news/grok-4-1-fast, 2025.

A. Yang, A. Li, B. Yang, et al. Qwen3 technical report. *arXiv preprint arXiv:2505.09388*, 2025. URL https://arxiv.org/abs/2505.09388.

Z. Yang, S. Yang, L. Hu, and D. Wang. Word recovery in large language models enables character-level tokenization robustness. *arXiv preprint arXiv:2603.10771*, 2026. URL https://arxiv.org/abs/2603.10771.

A. Zhuo, X. Ning, N. Li, Y. Wang, and P. Lu. On the ability of LLMs to handle character-level perturbations: How well and how? *arXiv preprint arXiv:2510.14365*, 2025. URL https://arxiv.org/abs/2510.14365.

A Limitations

Indirect mechanism evidence. Our two-modes hypothesis rests on behavioral observations and tokenization statistics rather than internal model states. A direct mechanistic account would require access to attention patterns or layer-wise activations, none of which are available through black-box APIs. The entropy analysis provides indirect support that is consistent with the hypothesis but does not confirm it causally; future work with open-weight models could probe internal representations directly.

Model coverage and proprietary models. Only three of eight evaluated model families exhibit a clear U-shape. We cannot determine whether the others fail to do so due to training data composition, architectural choices, tokenizer design, or safety-related output filtering. All evaluated models are proprietary, which limits reproducibility and makes it impossible to control for training data. Replication with open-weight models of documented training composition (e.g., LLaMA, Mistral, or Qwen open variants) would allow more controlled comparisons and is an important direction for future work.

Domain and task coverage. Although we evaluate word-boundary fragmentation across absence detection, NIAH-style insertion detection, and a direct math reasoning task, our coverage remains limited. The strongest evidence comes from long-context document-comparison settings, especially absence detection, where exact lexical alignment is central to the task. Our math reasoning experiment extends beyond document comparison, but only to GSM8K-style problems and shows that the effect can be model- and task-dependent. Whether the Text Uncanny Valley appears in other task types, such as question answering, summarization, reading comprehension, or code generation, remains unknown. These tasks impose different forms of lexical alignment pressure and may exhibit different sensitivity to word-boundary corruption. Similarly, we fix the omission and insertion rates at $p = 0.1$ for the document-comparison tasks; although we verified that varying this rate does not substantially change the U-shaped curve, a systematic study across target rates is beyond the scope of this work.

Perturbation scope. We study only intra-word space insertion as the corruption mechanism. Real-world OCR errors include character substitution, deletion, transposition, and merging, which may interact differently with absence detection and may or may not produce non-monotonic performance curves. Our analysis is also conducted at the whitespace-delimited word level rather than the subword token level; an intra-token analysis studying how fragmentation interacts with tokenizer boundaries directly could yield finer-grained mechanistic insight and is a promising direction for future work. The thinking-mode evaluation is additionally limited to two model families on one domain, so the observed asymmetry between GPT-5.2 and Gemini 3.0 Flash should not be generalized without broader investigation.

Generalisability beyond absence detection. We evaluate word-boundary fragmentation beyond absence detection through a NIAH-style insertion detection task (Appendix C) and a direct GSM8K math reasoning task (Appendix B). The NIAH-style task shows a weaker but still observable U-shaped effect, consistent with our argument that absence detection is a particularly sensitive testbed because it requires exact lexical alignment between two document versions. The math reasoning task further suggests that the effect is model- and task-dependent: Gemini 3.0 Flash exhibits a clear U-shape, while GPT-5.2 and Claude 4.5 Haiku remain near ceiling. These results extend the phenomenon beyond absence detection, but they do not establish full generality. Whether the Text Uncanny Valley appears in other task types, such as question answering, summarization, reading comprehension, or code generation, remains unknown. Future work should test whether the U-shaped curve generalizes to broader long-context alignment and text-processing tasks.

Statistical power and computational cost. We evaluate 100 documents per domain with three fragmentation seeds. While sufficient to reveal consistent U-shaped trends, this limits the statistical power of fine-grained analyzes such as precisely locating the valley bottom or quantifying its depth across document subsets.

Scaling to larger samples was not feasible given the structure of our evaluation protocol. Each document requires 11 separate API calls, one per `word_fragmentation_rate` level, and each prompt is approximately twice the length of the original document, because the AbsenceBench

task format requires both the original and modified contexts in the same prompt. Our documents average several thousand tokens in length; across 100 documents, 11 `word_fragmentation_rate` levels, 3 model families, 3 domains, and 3 fragmentation seeds, the main experiments alone require approximately 29,700 API calls ($100 \times 11 \times 3 \times 3 \times 3$), not counting NIAH, ICL, fixed-slot, and thinking-mode variants, which add further thousands. Many documents, especially in the legal domain, are long enough to require model context windows of 32K tokens or more. The combined effect of long prompts, many API calls per document, and high per-call latency made the full evaluation both time-consuming and costly, and was conducted at the limit of our available computational resources.

B Math Reasoning Under Fragmentation

We apply the same random-slot fragmentation protocol (Algorithm 1) to individual GSM8K problems to test whether the Text Uncanny Valley generalizes beyond absence detection.

Setup. We randomly sample 500 problems from the GSM8K test split (seed 42) and evaluate each model on each problem independently at eleven `word_fragmentation_rate` levels $(0.0, 0.1, \ldots, 1.0)$. Each API call consists of a single fragmented problem; thinking mode is disabled for all models to isolate tokenization level effects. Accuracy is measured by exact numerical match, with tolerance for minor formatting differences (e.g., $13.00 = 13$), using the pattern `The answer is #### [result]` as the primary extraction target, with fallback to the last number in the response. Both the input context (a single problem) and the expected output (a single number) are substantially shorter than in the absence detection experiments, which use 80-problem concatenated documents.

Prompt. Each model receives the following prompt, where `{question}` is replaced with the fragmented problem text:

Table 1: Prompt template used in the math reasoning experiment. The placeholder `{question}` is replaced with the fragmented problem text at each `word_fragmentation_rate` level.

User Message
`Question: {question}` `Solve the problem step by step and end with 'The answer is #### [result]'.`

C NIAH Results Under Fragmentation

We evaluate word-boundary fragmentation on a NIAH-style task using the same AbsenceBench framework [Fu et al., 2025], adapted to detect *added* rather than missing lines. Specifically, each instance presents the model with both the original document and a modified version to which extra lines have been inserted; the model must identify exactly which lines were added, scored by Micro-F1. The prompt template is provided below (Table 2).

Table 2: Prompt template used in the NIAH control experiment (Appendix C). Unlike the main prompt (Table 5), this variant asks the model to identify *added* lines rather than *missing* ones. No ICL prefix is used.

System Prompt

```
You are helping someone identify components that were added to a
{document_type}.  The person will provide their version of the {document_type},
but they may have added some random lines that were not in the original
text.  Your task is to identify exactly which lines are not in the original
{document_type}.  List only the extra lines, nothing else.
```

User Message

```
Here is the complete original {document_type}:
{original_context}
Now, here is my recitation with some extra lines that were not in the original
{document_type}:
{modified_context}
What lines did I add to the {document_type}?  Please list only the extra
lines, nothing else.
```

We apply the same eleven `word_fragmentation_rate` levels across all three model families and three domains. The U-shaped effect is substantially weaker than in absence detection. On GitHub PRs, all three models remain near-ceiling with no discernible U-shape. On legal documents, mild non-monotonic variation is visible but not pronounced. On mathematical reasoning, Claude 4.5 Haiku shows a more visible U-shape (from approximately 0.95 to 0.75 and back), while GPT-5.2 and Gemini 3.0 Flash remain largely stable. Overall, the effect is attenuated compared to absence detection, consistent with our argument that absence detection is a more sensitive testbed: it operates far from ceiling and requires exact lexical alignment across two document versions, amplifying the impact of tokenization disruption.

Needle design. For each domain, we construct 100 needle sentences whose length distribution matches the per-line length distribution of the corresponding dataset. The needles are domain-appropriate text that does not appear in the original datasets: synthetic legal clauses for legal documents, synthetic code diff hunks for GitHub PRs, and synthetic math word problems for GSM8K. For each document, we sample a set of synthetic needle lines so that the number of inserted lines matches the insertion rate used in the main experiments. Needles are sampled from a domain-specific pool and inserted at random positions. Crucially, the inserted needle is subjected to the same `word_fragmentation_rate` fragmentation as the surrounding document, ensuring that the model must detect an added fragment-level span rather than a clean insertion.

Table 3 shows representative needle examples at their respective fragmentation levels.

Table 3: Representative needle examples at domain-specific `word_fragmentation_rate` levels. Needles are domain-appropriate synthetic text, subjected to the same fragmentation as the surrounding document.

Domain (`word_fragmentation_rate`)	**Needle example**
GitHub PRs (0.3)	`dif f - -git a/src / Illum in ate/A uth /Acce s s / G at e .p hp b/src/... @@ -1 42,6 +154,12 @@ p rot ect ed fu n ction r esolveAuthC allba ck... - r e turn $ thi s->co ntaine r->make($c a l lba ck)- > h a n d l e($user , ...$a rgu men ts);`
Legal Docs (0.5)	`Not w ith s ta n d i ng t h e p ro visi o ns of S ect i o n 4 .2 , Va n te d g e C a pi t a l sh a l l r em i t a q ua r terl y i n frastru ct u r e o pti m izat i on pa y m e nt o f $ 1 8, 4 5 0 t o th e p r ovid er [...] T h is M a s te r A g ree m e n t s h al l b e a ut om a t i call y ex tend e d f o r a n ad di ti o n al ni n e -m on t h t erm u nles s [...]`
Math (0.7)	`S a r a h h as a c o l le c ti on o f 5 0 v in t age p os t a g e s t a m p s . S h e d eci de s t o s e l l 12 of t he m at a n a u c t i o n to buy 8 r a re on e s . H er gra n df a the r t h e n g ift s h e r h is ow n co l l e c ti on w h i c h is thre e tim e s t h e si ze o f Sa rah ' s c u r r e n t set . H ow m any s tam ps d o e s s he h a v e i n t o t al n o w ?`

D Results for All Evaluated Models

We evaluated eight model variants in total. As noted in Section 4.1, only Gemini 3.0 Flash, GPT-5.2, and Claude 4.5 Haiku consistently exhibit the Text Uncanny Valley. This appendix provides the full Micro-F1 curves for the remaining variants.

Non-U-shape models (legal documents). Figure 9 shows results for DeepSeek-V3, Grok-4.1-Fast, and Qwen3-Plus on legal documents. Grok-4.1-Fast shows largely monotonic decline without a clear rebound. Qwen3-Plus exhibits irregular curve shapes with no consistent trend across fragmentation rates; its overall performance is poor, and API calls were substantially slower and more costly than other models, which precluded its inclusion in further experiments. DeepSeek-V3 exhibits an important anomaly: as `word_fragmentation_rate` increases, certain documents consistently trigger internal errors or refusals, and at `word_fragmentation_rate` $= 1.0$ the model is almost entirely non-functional on this domain. We conjecture this reflects an internal content-filtering mechanism that is triggered by the unusual character distribution of fully fragmented text. Due to these errors, we omit the `word_fragmentation_rate` $= 1.0$ data point for DeepSeek-V3 on legal documents from all figures and analyzes.

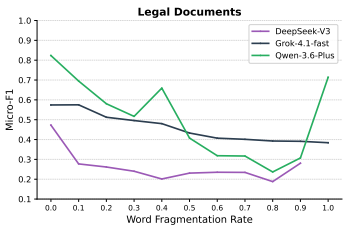

Figure 9: Micro-F1 as a function of `word_fragmentation_rate` for DeepSeek-V3, Grok-4.1-Fast, and Qwen3-Plus on legal documents, with all three models overlaid. DeepSeek-V3 results at `word_fragmentation_rate` $= 1.0$ are omitted due to consistent API errors at that fragmentation level.

E Experimental Details

E.1 GSM8K document structure

Table 4: Structure of a GSM8K document. Each document concatenates 80 problems; questions and answers are each split into individual lines.

Line index	Content
1	Problem 1, question line 1
...	...
k	Problem 1, question line k
k+1	Problem 1, answer line 1
...	...
N	Problem 80, answer line (last)

E.2 Prompt template

Table 5: Prompt template used in all experiments. Placeholders in blue are filled at runtime. In our experiments, `{document_type}` is replaced with `Legal Documents`, `Github PRs`, or `Mathematical Reasoning` depending on the domain. The ICL prefix is prepended only when ICL is enabled (Section 5.1).

System Prompt

```
You are helping someone identify missing components from a {document_type}.
The person will provide their version of the {document_type}, but they may
have missed some lines.  Your task is to identify exactly which lines are
missing from their version.  List only the missing lines, nothing else.
```

User Message

(Optional ICL prefix:) `Below are some examples of the task: {icl_examples} --`

```
Here is the complete original {document_type}: {original_context}
Now, here is my recitation which may be missing some lines:
{modified_context}
What lines did I miss?  Please list only the missing lines, nothing else.
```

E.3 Fragmentation examples

Table 6: Effect of word-boundary fragmentation at four `word_fragmentation_rate` levels on a legal document excerpt. Only intra-word slots receive inserted spaces; inter-word spaces and punctuation are unchanged.

`word_fragmentation_rate`	Text excerpt
0.0	This Promotion Agreement (the "Agreement") is dated as of January 26, 1998 between CNET, Inc. ("CNET") and Cyberian Outpost, Inc. (the "Company"). [...]
0.1	This Promoti on A greemen t (the "Agreement") is dated as of January 26, 1998 between CNET, I nc. ("CN ET") and Cyberian Ou tpost, Inc. (the "Company"). [...]
0.5	T h is P r om oti o n A greem e n t (th e "A g re e m e n t") is dated a s of J an ua r y 26, 1998 b e twe en CN ET, I nc. ("CN ET") a n d Cy be r i an O u t p o st, I n c. (th e "Com p an y"). [...]
1.0	T h i s P r o m o t i o n A g r e e m e n t (t h e "A g r e e m e n t") i s d a t e d a s o f J a n u a r y 2 6 , 1 9 9 8 b e t w e e n C N E T , I n c . ("C N E T") a n d C y b e r i a n O u t p o s t , I n c . (t h e "C o m p a n y"). [...]

E.4 ICL example template

Table 7: ICL prefix prepended to the user message. Each example shows a fragmented document, a modified version with lines removed, and the correct answer. Only Example 1 is shown in full.

ICL prefix prepended to User Message

```
Below are some examples of the task:

Example 1:
Here is the complete original document:
Th e fund amen tal pr incipl es of qu ant um co mpu ting inv olve s uperpo
sition .
Th ese p henomen a allow f or com putatio nal spe eds f ar excee ding cl assic
al ar chitectu re .
Imple ment ing r obust er ror co rrecti on rem ains a s ignific ant h urdle f
or res earchers .
Cr yogen ic en vironmen ts a re nece ssary t o ma intain t he stabili ty o f
su percon ducting q ubits .
[...]

Now, here is my recitation which may be missing some lines:
Th e fund amen tal pr incipl es of qu ant um co mpu ting inv olve s uperpo
sition .
Th ese p henomen a allow f or com putatio nal spe eds f ar excee ding cl assic
al ar chite ctu re .
Cr yogen ic en vironmen ts a re nece ssary t o ma intain t he stabili ty o f
su percon ducting q ubits .
[...]

What lines did I miss?  Please list only the missing lines, nothing else.
Answer:
Imple ment ing r obust er ror co rrecti on rem ains a s ignific ant h urdle f
or res earchers .

--
Example 2:  [...]
--
Example 3:  [...]
```

```
--
```
(Standard user message follows here.)

E.5 Fragmentation procedure

Algorithm 1 describes the random-slot fragmentation used in the main experiments. Algorithm 2 describes the fixed-slot variant used in Experiment B (Section 5.2).

Algorithm 1 Random-slot fragmentation

Require: Document lines L, insertion probability $p \in [0, 1]$
Ensure: Fragmented lines L', measured `word_fragmentation_rate` $\in [0, 1]$

```
inserted ← 0; eligible ← 0
for each line ℓ ∈ L do
    ℓ′ ← ""
    for i = 0 to |ℓ| − 1 do
        ℓ′ ← ℓ′ + ℓ[i]
        if i + 1 < |ℓ| and ℓ[i] ∉ whitespace and ℓ[i + 1] ∉ whitespace then
            eligible ← eligible + 1
            if Bernoulli(p) = 1 then
                ℓ′ ← ℓ′ + "  "; inserted ← inserted + 1
            end if
        end if
    end for
    Append ℓ′ to L′
end for
return L′, word_fragmentation_rate = inserted/ max(eligible, 1)
```

Algorithm 2 Fixed-slot fragmentation (first-slot variant)

Require: Document lines L, insertion probability $p \in [0, 1]$
Ensure: Fragmented lines L', measured rate

```
inserted ← 0; eligible ← 0
for each line ℓ ∈ L do
    Split ℓ into non-space sequences S = [s_1, s_2, ...] and whitespace tokens
    for each sequence s ∈ S do
        if |s| ≥ 2 then
            eligible ← eligible + (|s| − 1)                ▷ count all gaps in sequence
            if Bernoulli(p) = 1 then
                Insert "  " after s[0]                     ▷ first slot only
                inserted ← inserted + 1
            end if
        end if
    end for
    Reconstruct ℓ′ from modified sequences and original whitespace
    Append ℓ′ to L′
end for
return L′, rate = inserted/ max(eligible, 1)
```